J Solid State Electrochem (2011) 15:829–836
DOI 10.1007/s10008-010-1157-y

ORIGINAL PAPER

Nitric oxide measurement in biological and pharmaceutical samples by an electrochemical sensor

Fang Wang · Xiaocui Deng · Wei Wang · Zilin Chen

Received: 1 February 2010 / Revised: 28 June 2010 / Accepted: 25 July 2010 / Published online: 11 August 2010

Abstract A nitric oxide (NO) electrochemical sensor was developed via one-step construction of gold nanoparticles (GNPs)–chitosan (CS) nanocomposite sensing film on a glassy carbon electrode (GCE) surface. This method is very simple and convenient. The GNPs–CS film which is controllable and stable exhibits catalytic activity to NO oxidation. The anodic peak potential significantly shifted negatively compared with that at bare GCE. The high sensitivity and good stability of developed method have been coupled to a wide linear range from 3.60×10^{-8} to 4.32×10^{-5} M for the quantitative analysis of NO. The detection limit of 7.20 nM is much lower than the vast majority of reported methods. This NO sensor has been successfully applied to NO measurement in biological and pharmaceutical samples. Real-time amperometric data show that the addition of L-arginine (L-Arg) can cause a slow release of NO from a whole rat kidney with a maximum concentration of ca. 150 nM. The concentration of NO monitoring from the drug sample was calculated to be ca. 1.60 μM.

Keywords Electrochemical sensor · Gold nanoparticles · Nitric oxide detection · Pharmaceutical analysis

Introduction

Nitric oxide (NO) is a small, gaseous, paramagnetic radical with biological activity. It can be dissolved in solutions (or tissue/body fluid) and diffuse to neighboring cells, bacteria, and viruses. NO is synthesized within cells by an enzyme NO synthase (NOS) and was identified as the endothelial-derived relaxing factor (EDRF) in 1987 [1, 2]. It has been found that NO plays an ubiquitous role in the control of physiological functions throughout the body. On one hand, it has an enormous range of beneficial functions in organisms, including regulation of vascular tone, ventilation, hormone secretion, inflammation, immunity, and neurotransmission. On the other hand, NO is also suspected to be cytotoxic or cytostatic to host cells and to act as a toxic radical [3-7]. McCann once suggested that excessive production of NO, in the central nervous system and its related glands, might be the most important factor in aging of some body structures [8]. Now more and more evidences occur for this NO hypothesis of aging [8]. For a more detailed understanding of NO's physiological and pathological effects as well as the biological functions, great efforts have been put into developing, or modifying, specific measurement techniques to suit its measurement in biological samples, especially in vivo measurements [9].

NO persists in solution for several minutes and in biological tissues (blood) for several seconds [10, 11]. So measurement of NO in biological tissues is very difficult and challenging. Taha has summarized different techniques and methodologies used in measuring NO in biological samples [9]. Those include gas- and liquid-phase chemiluminescence, electron spin resonance spectroscopy, UV-visible spectroscopy, fluorescence, electrochemical sensors, and reported cell assay [9]. It has been claimed that electrochemical methods are the most practical in measuring NO in biological samples due to small electrode size, in vivo capability, nondestructive properties, minimal or no reagents requirements, sensitivity, simplicity, and low cost. Moreover, electroanalytical methods can be operated with

F. Wang · X. Deng · W. Wang · Z. Chen (✉)
Department of Pharmaceutical Analysis, College of Pharmacy,
Wuhan University,
Wuhan 430072, China
e-mail: chenzl@whu.edu.cn

limited electrochemical knowledge [9]. Through the long-term development, diverse kinds of electrochemical methods with great progress have been constructed. More and more publications of NO electrochemical sensor appeared since report of the first electrochemical sensor for NO analysis in biological samples in 1989 [12], especially the fabrication of porphyrinic sensor [13].

Now most of researchers are focusing on the chemically modified electrode (CME)-based electrochemical sensor using kinds of materials [14]. Nanomaterials are the most competitive because of their unique electrical and catalytic properties [15]. They have been widely used to improve the performance of NO sensors. Carbon nanotubes (CNTs) is the most commonly used [16-24], for example, it has been used to modify the surface of a carbon fiber microdisk electrode to construct a highly sensitive NO sensor. Constructed sensor was successfully applied to the measurement of NO released from single isolated human umbilical vein endothelial cells (HVECs) [16]. Except for CNTs, other nanoparticles or nanocompounds have either been used as sensing and catalytic element for NO sensor development such as nano-Al_2O_3 [25], TiO_2/MWCNTs [17], platinum nanoparticles/CNTs [18], polymer/CNTs [19], TiO_2–Au nanocomposite [26], PVP-coated iron nanocrystals [27], copper nanoparticle [28], clay nanoparticles [29], and Au nanoparticles [30-34]. These sensors are provided with either not high enough sensitivity or complexity of the production process. The main aim of investigation here is to improve the detection sensitivity and operation convenience of NO measurement in biological tissues by employing a one-step modification procedure to prepare NO sensor. Nanoparticles (intermediate between the size of small molecules and that of bulk metal) would display electronic structures, reflecting the electronic band structure of the nanoparticles, owing to quantum-mechanical rules [35]. Gold nanoparticles (GNPs) are faradaically inactive, and they can act as electron antennae to facilitate electron transfer via efficiently funneling electrons between the electrode and the electrolyte [36, 37]. Chitosan (CS) can be used to form hydrogel for immobilization of GNPs referring to the refs [38, 39]. Based on the excellent catalytic activities of GNPs and good film-forming ability of CS [40-42]. GNPs embedded in CS hydrogel would show remarkable catalytic activity to electrochemical oxidation of NO.

In present work, therefore, a simple and controllable electrodeposition method for preparation of a electrochemical NO sensor was proposed and performed by one-step electrochemical deposition in solution containing tetrachloroauric (III) acid ($HAuCl_4$) and CS. Several key operational parameters affecting the electrochemical response of nanostructured sensing film were examined and optimized, such as deposition conditions, pH values, and detection conditions. Furthermore, the performance of constructed sensor, including the sensitivity, linear range, and response time, was presented and discussed. Finally, this sensor was successfully applied to NO measurement in biological and pharmaceutical samples.

Experimental

Chemicals

Tetrachloroauric (III) acid ($HAuCl_4$) was purchased from Sinopharm Chemical Reagent Co., Ltd (Shanghai, China) and dissolved in water (Chongqing Qianyan Water Disposal Equipment Co., Ltd., Chongqing, China) to form the concentrations of 3.76×10^{-3} M. Trisodium citrate dihydrate ($Na_3C_6H_5O_7{\cdot}2H_2O$) was obtained from Shanghai Shisi Haowei Chemical Industry Co., Ltd. (Shanghai, China). CS stock solution (10.00 mg/mL) (bought from Shanghai Ruji Biological Technology Development Co., Ltd (Shanghai, China)) was prepared by 0.05 M acetic acid and stored at 4 °C. Nitric oxide (NO) standard solution was freshly prepared by dropping H_2SO_4 (2.00 M) into deoxygenated $NaNO_2$-saturated solution slowly. The generated gas was collected by dissolving it in deoxygenated water to prepare saturated NO stock solution after bubbling along the 30% NaOH solution twice and then deionized water once to remove the interferential substances produced by trace of oxygen. L-arginine (L-Arg) from Shanghai Ruji Biological Technology development Co., Ltd. (Shanghai, China) was dissolved in water to form a concentration of 0.10 M. The concentration of NO in saturated stock solution is 1.80 mM at 25 °C [43]. The pH of phosphate-buffered saline was adjusted with 0.10 M HCl or NaOH. All other chemicals were of analytical grade quality and used without further purification. The water used was deionized water.

As to the biological sample, male mice (km, no. 00003186) were used. The rat was sacrificed by decapitation several minutes before detection. The kidney was immediately excised and stored in cold Euro-Collins solutions in fridge for experiments.

The powder sample of sodium nitroprusside (SNP) was provided by Wuhan Humanwell Pharmaceutical Co., Ltd. SNP sample was prepared by dissolving in deionized water with a concentration of 0.40 M before the experiments.

Apparatus and methods

All voltammetric determinations were performed on a CHI 830B electrochemical analyzer (CH Instrument Co., Shanghai, China). All experiments were carried out in a conventional electrochemical cell. The electrode system contained a glassy carbon working electrode (GCE from CHI, 3.00 mm in diameter), a platinum wire counter electrode, and a saturated calomel reference electrode (SCE). A single

compartment cell was used. All potentials were measured versus the SCE. Scanning electron microscopy (SEM) was done with a Hitachi X-650 microscope. All experiments were performed at room temperature (25±1 °C). For the deoxygenated experiments, the electrolyte was bubbled with high-purity (99.999%) nitrogen for 15 min and maintained nitrogen condition during the experiments.

Preparation of NO sensor

Firstly, 10.00 mg/mL of CS and 3.76×10^{-3} M $HAuCl_4$ solution were mixed together according to the ratio of 20:1 (*v:v*), and then was shaken well. Prior to experiments, a glassy carbon electrode (GCE) was mechanically polished with wetted microcloth containing 0.05-μm alumina powder, and then carefully cleaned in ethanol and water by ultra-sonication bath, each for 10 s. The NO sensor was prepared by one-step electrochemical deposition in solution containing $HAuCl_4$ and CS on pretreated GCE at an applied potential of −1.00 V for 60 s (GCE/CS–GNPs). The CS-modified electrode was prepared in the same way without $HAuCl_4$ (GCE/CS). The prepared electrodes were rinsed with deionized water to remove unbounded materials from the electrode surface for use.

Analysis procedures

At the beginning of the experiment, the GCE/CS–GNPs was evaluated by successive cyclic voltammetric sweeps in 0.10 M phosphate-buffered saline (PBS) (between 0.00 and 1.20 V at 100 mV/s) to get a stable voltammetric response. Five milliliters of 0.10 M PBS was subsequently used as the supporting electrolyte, and the electrochemical behavior of NO was mainly investigated by differential pulse voltammetry (DPV). As far as NO measurement was concerned, a conventional amperometric method was introduced at 0.85 V under a stirred condition. The NO-saturated solution was added into the PBS after steady electrochemical responses were obtained. The kidney experiments were carried out referring to the following ref. [44]. The electrode was positioned in buffer solution. The kidney was close to the working electrode surface, and the solution was not agitated.

Results and discussion

Operational parameters for GCE/CS–GNPs preparation

In order to obtain the best performance of NO sensor, operational parameters for GCE/CS–GNPs preparation was investigated using 1.44×10^{-6} M NO as a probe. Figure 1 shows the effects of experimental conditions on electrochemical characteristics of the film, such as electrodeposition potential (Fig. 1a), time (Fig. 1b), and pH of electrolyte (Fig. 1c). It is known that the CS hydrogel film was formed by a pH shift-induced deposition of CS onto the electrode surface [45]. If a highly enough negative potential was exerted on the working electrode, the H^+ near the cathode was reduced to H_2 at the cathode and released, and then the pH near the cathode surface gradually increased. While the pH was higher than 6.30, CS became insoluble and then formed a film on the electrode surface [46]. In general, the release rate of H_2 is dependent on the applied deposition potential. When the potential shifted positively, the rate of H^+ generation became slow and then the localized pH in the vicinity of the electrode surface increased slowly. If the rate decreased greatly, it was very difficult to produce the CS film on electrode surface even after a long time. Certainly, excessive H^+ evolution would produce a breakable film or a thick film blocking the electron transfer. The results are similar to those reported results [46, 47]. Therefore, −1.00 V was chosen as the optimal potential for GCE/CS–GNPs preparation according to Fig. 1a.

The effects of electrodeposition time on electrochemical response of NO are demonstrated in Fig. 1b. The peak current of NO increases with the increase of time and reaches maximum at 60 s and then drops. It may be that the deposition time can influence the thickness of CS–GNPs film. Based on the results in Fig. 1b, 60 s has been chosen as the optimal electrodeposition time.

The pH of solution for deposition will influence the electrochemical characteristics of the film and then the current response of NO. It was known that CS cannot be dissolved in acetic acid if its pH is larger than 6.0. So the 0.05 M acetic acid (pH<6.0) was chosen as supporting electrolyte. The pH was adjusted with HCl. The effects of pH on NO current were investigated and shown in Fig. 1c. The data suggest that best current response of NO could be obtained at pH=2.0. CS can act as metal-complexing agent. Probably, strong acid media can provide special environment for the interaction between CS hydrogel and GNPs during the electrodeposition process, so the GCE/CS–GNPs was prepared at −1.00 V for 60 s in 0.05 M acetic acid (pH=2.0).

Lastly, SEM was used to characterize the surface morphologies of CS–GNPs films as shown in Fig. 1d. It could be seen that GNPs was well fixed and uniformly dispersed in the CS hybrid film. No aggregation of them was observed. It suggested that this method embedding in situ GNPs in CS hydrogel was preferable.

Electrochemical behavior of NO at GCE/CS–GNPs

The electrochemical behaviors of NO at different electrodes in 0.10 M PBS (pH=7.4) were investigated by DPV, and the results are illustrated in Fig. 2. Curve c in Fig. 2 shows

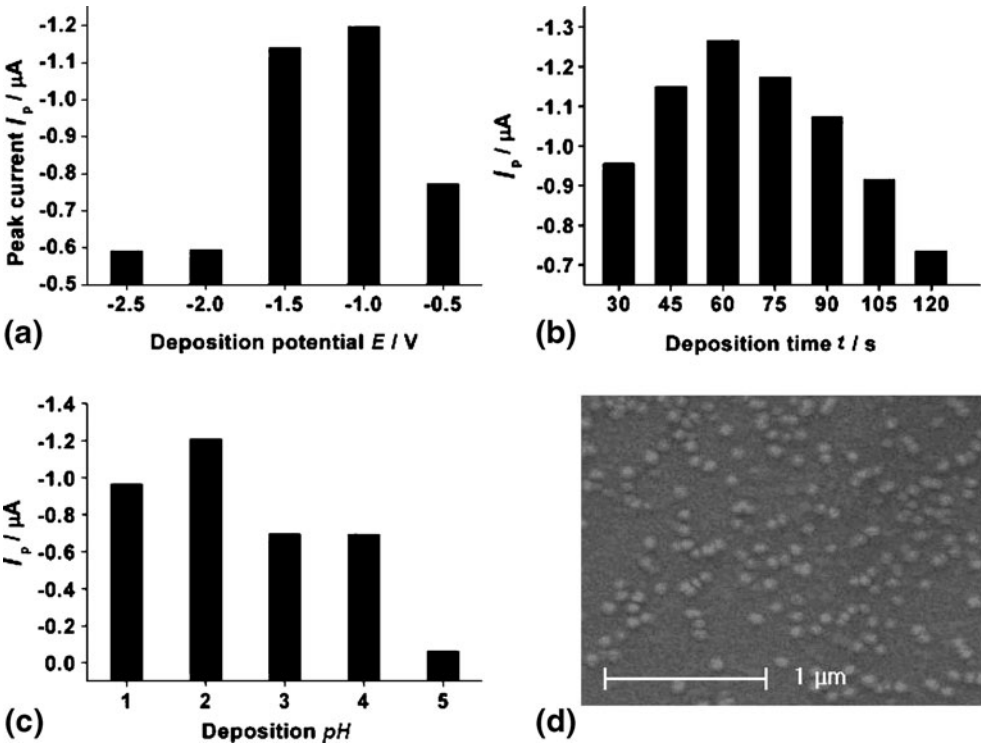

Fig. 1 The dependence of peak current of 1.44×10^{-6} M NO by DPV in 0.10 M PBS (pH=7.4) on deposition conditions of Au_{nano}–CS film including **a** potential (pH=2.0, 60 s), **b** time (pH=2.0, −1.0 V), **c** pH (60 s, −1.0 V), and **d** SEM (20.0 kV, 20000×) image of Au_{nano}–CS film on GCE (pH=1.0, −1.0 V, 60 s)

the current response of GCE/CS–GNPs in the absence of NO after that the sensor was evaluated by successive cyclic voltammetric sweeps. There is unobvious peak due to the poor response of Au_{nano} oxidation. Addition of 3.60×10^{-6} M NO results in the appearance of a new oxidation at about 0.73 V, accompanied by great increase of current. This peak is attributed to oxidation of NO, which is demonstrated in Fig. 2 (curve a); however, only a broad oxidation peak at about 1.10 V appears at bare GCE in the presence of NO shown as curve b in Fig. 2. Based on these discussions, GNPs shows great enhancement effects on the electrochemical oxidation of NO including the negative shift of peak potential and increase of peak current, which was due to excellent catalytic activity of GNPs and roughened conductive-high-surface area of CS–GNPs film [26, 43, 48]. In view of the cyclic voltammograms of NO at three above-mentioned different electrodes (the data were not listed), it is sure that electrochemical oxidation of NO at these electrodes is a totally irreversible process. There is no reduction peak on the reversal scan from 1.20 to 0.20 V. As a result, a method for NO determination was developed considering the highly sensitive response of GCE/CS–GNPs to NO oxidation.

Calibration curve and interferences

Conventional amperometric method was used to characterize the current response upon the successive addition of NO as shown in Fig. 3. The current of NO at a very low concentration proved that this electrochemical method has high sensitivity and low detection limit. The calibration curve for NO detection was obtained by Fig. 3 and displayed in Fig. 4. The response of GCE/CS–GNPs revealed good linear behavior in the concentration range from 3.60×10^{-8} to 4.32×10^{-5} M for the quantitative analysis of NO with a limit of detection of 7.20×10^{-9} M.

In order to evaluate the anti-interference ability of the GCE/CS–GNPs, the current responses of 7.20×10^{-6} M NO was analyzed with coexist of some small biomolecules and inorganic ions. The results showed that 100-fold Ca^{2+}, Mg^{2+}, Fe^{3+}, 50-fold Zn^{2+}, and 6.0×10^{-6} M uric acid almost

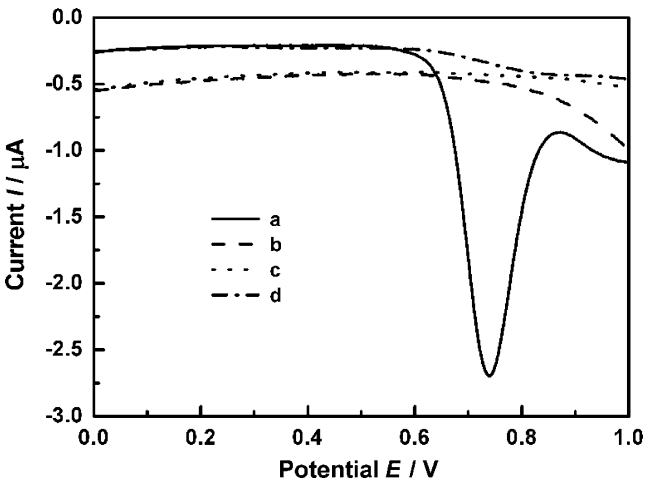

Fig. 2 Differential pulse voltammograms of bare GEC (**b**, **c**) and Au_{nano}–CS film modified GCE (**a**, **d**) in absence (**c**, **d**) and presence (**a**, **b**) of 3.60×10^{-6} M NO in 0.10 M PBS (pH=7.4)

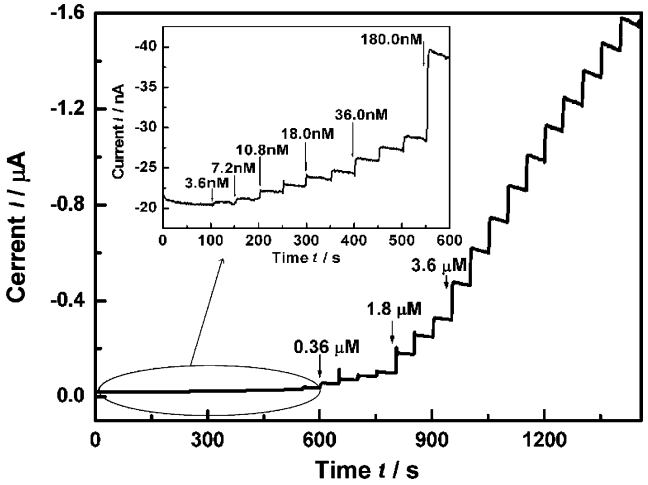

Fig. 3 Amperometric response of NO at Au_{nano}–CS film modified GCE at 0.85 V. *Inset* is the magnified graph of NO response between 0 and 600 s

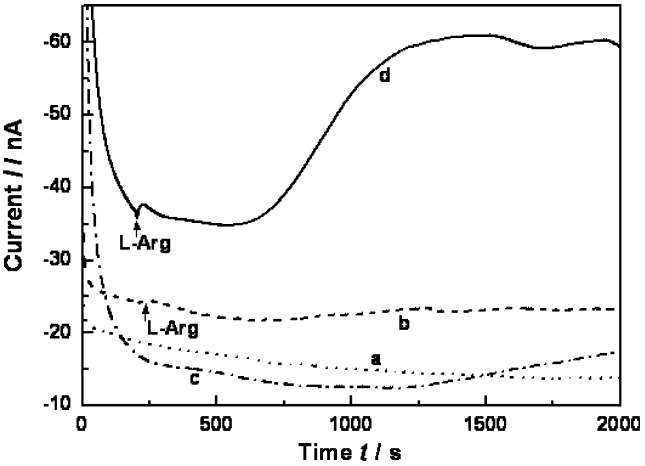

Fig. 5 Monitoring NO release from PBS (**a**), PBS with addition of L-Arg (**b**), PBS and kidney (**c**), PBS and kidney with addition of L-Arg (**d**). Applied potential, 0.85 V

have no influence on the detection of NO (signal change below 8.00%); however, a small amount of dopamine and ascorbic acid would result in the obvious signal change. It was considered that dopamine and ascorbic acid as strong reductants could influence the electroactivity of Au nanoparticles. Moreover, the adsorption behavior of products by dopamine and ascorbic acid oxidation on the GCE/CS–GNPs surface would occupy the active sites of sensing film, and then current response of NO was decreased. All discussions prove that this senor has certain anti-interference ability.

Stability, repeatability, and productivity

Stability, repeatability, and productivity are key parameters for measurement of sensor performance. In present work, the current response of NO can remain 92.00% of original value after that the GCE/CS–GNPs was kept in air for 8 days. At the same time, the relative standard deviation (R.S.D.) for eight-time parallel detections of 7.20×10^{-6} M NO with the same GCE/CS–GNPs was obtained to be of 7.10% and that with eight different electrodes is 4.60%. These data suggest that developed GCE/CS–GNPs exhibits good stability and satisfactory repeatability, as well as excellent reproducibility. This method provided a new chance for the determination of NO in biological tissues.

NO release from biological tissue and medicine model

It has been found that the synthesis of NO in the body is involved in the reaction of various nitric oxide synthase (NOS) with L-Arg in the presence of trace O_2 [44, 49-53].

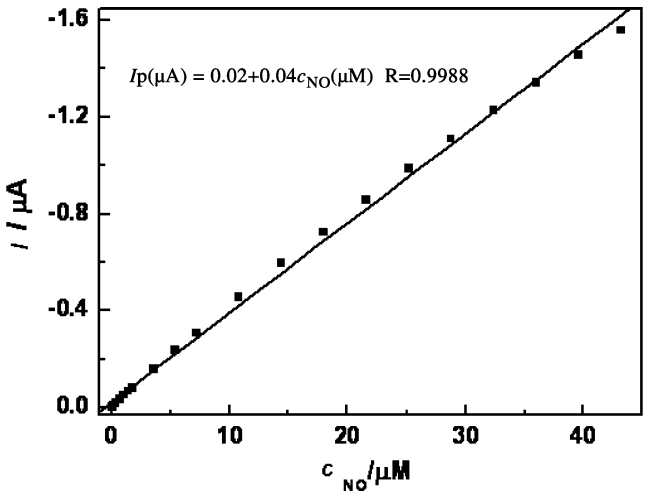

Fig. 4 Calibration curve for NO in 0.10 M PBS at Au_{nano}–CS film modified GCE. Applied potential, 0.85 V

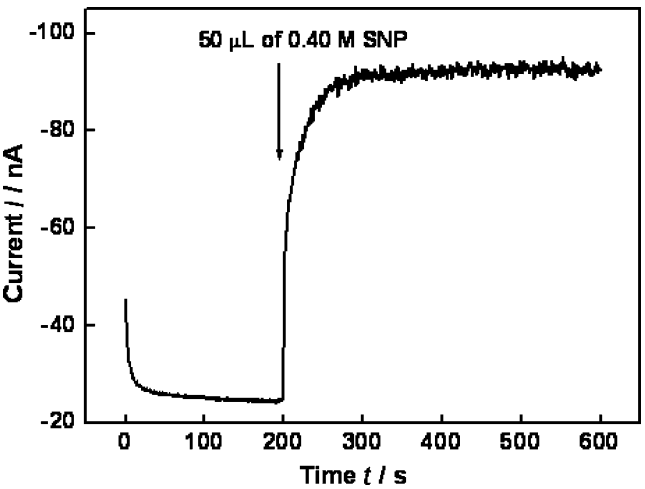

Fig. 6 Graphical result for the NO release from sodium nitroprusside samples. Applied potential, 0.85 V

Table 1 NO detection from 4 mM sodium nitroprusside

Sample	Current (nA)	Detected NO (μM)	Average (μM)	R.S.D (%)
1	−67.36	1.52	1.60	5.32
2	−70.85	1.69		
3	−69.09	1.60		

There is increasing evidence that endothelium-derived NO is tonically synthesized within the kidney and that NO plays a crucial role in the regulation of renal hemodynamics and excretory function [49, 50], so monitoring the NO concentration in kidney is of great importance. Here, fabricated GCE/CS–GNPs was applied to NO monitoring from rat kidney, and the results were demonstrated in Fig. 5. It is clear that no apparent NO current response can be observed without kidney or L-Arg in the PBS containing trace O_2 (curve a, b, and c in Fig. 5); however, remarkable change of amperometric current can be detected after the addition of L-Arg into PBS containing a whole kidney, suggesting the NO release from kidney (curve d). The concentration of NO released from the rat kidney sample was calculated to be ca. 150 nM. The long response time of about 500 s may be caused by the long-distance diffusion of L-Arg from the outside to the inside of kidney for reaction with NOS. This research provided a chance to construct perfect NO sensor for real-time NO measurement in vivo.

The GCE/CS–GNPs was also applied to NO monitoring from a powerful anti-hypertension medicine, sodium nitroprusside. Like all nitrates, sodium nitroprusside works by relaxing blood vessels. Once in the body, sodium nitroprusside is quickly broken down into NO. The breakdown of sodium nitroprusside to NO happens very quickly. In this experiment, when sodium nitroprusside solution sample was added in electrolyte, the response current changes in several seconds and reaches the maximal value during 100 s. The data was shown in Fig. 6 and Table 1. These results may help us get better understanding of pharmacokinetics of some medicines concerning NO release.

Concluding remarks

Based on the enhanced oxidation of nitric oxide (NO) at Au_{nano}–CS film modified electrode, a novel electrochemical NO sensor was fabricated by a simple and controllable electrodeposition method. Because of special electronic properties and excellent electrocatalytic ability of Au nanoparticles, this method exhibited high sensitivity, wide linearity, and low detection, as well as convenience, which was proved by the comparisons between this method and other different sensors from literatures in Table 2. Finally, the successful application of this sensor to monitoring NO from drugs and biological tissues proved that proposed simple method is feasible and highly efficient. Establishment of this platform could promote the research on the physiological and pathological effects as well as the biological functions of NO in life processes.

Acknowledgements This work was supported by the start-up fund for Luojia Chair Professorship of Wuhan University (nos. 306276216 and 306271159), the National Scientific Foundation of China (NSFC nos. 20775055, 30973672, 90817103, and 6080102.0), the Important National Science and Technology Specific Projects (no. 2009ZX09301-14), and the Fundamental Research Funds for the Central Universities.

Table 2 The comparison between this work and other publications about electrochemical NO sensor based on the Au nanoparticles-modified electrode for the detection of NO in aqueous solution

Conditions	Linear range (M)	Detection limit (nM)	Applications	Ref.
Gold hair microelectrode (0.80 V)	9.00×10^{-8}–3.50×10^{-5}	–	–	[30]
GCE/Nafion–Au_{nano} (0.90 V)	1.00×10^{-9}–1.00×10^{-8}	1.0	–	[31]
	5.00×10^{-4}–5.50×10^{-3}			
Hydrophilic Au_{nano} (0.86 V)	5.00×10^{-8}–1.00×10^{-5}	27.0	–	[32]
ITO/Au_{nano} arrays (0.93 V)	1.00×10^{-6}–5.00×10^{-4}	650.0	–	[33]
Red blood cells (RBCs)—Au_{nano} (−50 mV)	1.00×10^{-8}–1.00×10^{-6}	5.0	Raw blood	[34]
ITO/PE–Au_{nano} hydrid film	5.00×10^{-5}–1.00×10^{-4}	50,000	–	[54]
GCE/CS–Au_{nano} (0.85 V)	3.60×10^{-8}–4.32×10^{-5}	7.2	Rat kidney and sodium nitroprusside	Present work

References

1. Palmer R, Ferrige A, Moncada S (1987) Nitric oxide release accounts for the biological activity of endothelium-derived relaxing factor. Nature 327:524–526
2. Ignarro LJ, Buga G, Wood K, Byrns R, Chaudhuri G (1987) Endothelium-derived relaxing factor produced and released from artery and vein is nitric oxide. Proc Natl Acad Sci 84:9265–9269
3. Moncada S, Palmer RM, Higgs EA (1991) Nitric oxide: physiology, pathophysiology, and pharmacology. Pharmacol Rev 43:109–142
4. Gross SS, Wolin MS (1995) Nitric oxide: pathophysiological mechanisms. Annu Rev Physiol 57:737–769
5. Nathan C (1992) Nitric oxide as a secretory product of mammalian cells. FASEB J 6:3051–3064
6. Harrison DG (1997) Perspective series: nitric oxide and nitric oxide synthases. Cellular and molecular mechanisms of endothelial cell dysfunction. J Clin Invest 100:2153–2157
7. Yokozawa T, Chen CP (2001) Evidence suggesting a nitric oxide-scavenging activity for traditional crude drugs, and action mechanisms of sanguisorbae radix against oxidative stress and aging. J Amer Aging Assoc 24:19–30
8. Mccann SM, Licinio J, Wong ML, Yu WH, Karanth S, Rettorri V (1998) The nitric oxide hypothesis of aging. Exp Gerontol 33:813–826
9. Taha ZH (2003) Nitric oxide measurements in biological samples. Talanta 61:3–10
10. Beckman JS, Koppenol WH (1996) Nitric oxide, superoxide, and peroxynitrite: the good, the bad, and ugly. Am J Physiol Cell Physiol 271:C1424–C1437
11. Kelm M (1999) Nitric oxide metabolism and breakdown. Biochim Biophys Acta 1411:273–289
12. Shibuki K (1989) Calcium-dependent and ouabain-resistant oxygen consumption in the rat neurohypophysis. Brain Res 487:96–104
13. Malinski T, Taha Z (1992) Nitric oxide release from a single cell measured in situ by a porphyrinic-based microsensor. Nature 358:676–678
14. Alkire RC, Kolb DM, Lipkowski J, Ross PN (2009) Advances in electrochemical science and engineering: chemically modified electrodes, vol 11. Wiley-VCH, Weinheim, p 197
15. Arben M (2007) Nanobiomaterials in electroanalysis. Electroanalysis 19:739–741
16. Du FY, Huang WH, Shi YX, Wang ZL, Cheng JK (2008) Real-time monitoring of NO release from single cells using carbon fiber microdisk electrodes modified with single-walled carbon nanotubes. Biosens Bioelectron 24:415–421
17. Zhang L, Tian DB, Zhu JJ (2008) Direct electrochemistry and electrochemical catalysis of myoglobin–TiO_2 coated multiwalled carbon nanotubes modified electrode. Bioelectrochemistry 74:157–163
18. Zhang L, Fang Z, Zhao GC, Wei XW (2008) Electrodeposited platinum nanoparticles on the multi-walled carbon nanotubes and its electrocatalytic for nitric oxide. Inter J Electrochem Sci 3:746–754
19. Zheng DY, Hu CG, Peng YF, Yue WQ, Hu SS (2008) Non-covalently functionalized water-soluble multiwall-nanotubes through azocarmine B and their application in nitric oxide sensor. Electrochem Commun 10:90–94
20. Wu FH, Zhao GC, Wei XW (2004) Electrocatalytic oxidation of nitric oxide at multi-walled carbon nanotubes modified electrode. Electrochem Commun 4:690–694
21. Yang J, Pang FY, Zhang RY, Xu Y, He PG, Fang YZ (2008) Electrochemistry and electrocatalysis of hemoglobin on 1-pyrenebutanoic acid succinimidyl ester/multiwalled carbon nanotube and Au nanoparticle modified electrode. Electroanalysis 20:2134–2140
22. Tu WW, Lei JP, Ju HX (2008) Noncovalent nanoassembly of porphyrin on single-walled carbon nanotubes for electrocatalytic reduction of nitric oxide and oxygen. Electrochem Commun 10:766–769
23. Silva JF, Griveau S, Richard C, Zagal JH, Bedioui F (2007) Glassy carbon electrodes modified with single walled carbon nanotubes and cobalt phthalocyanine and nickel tetrasulfonated phthalocyanine: highly stable new hybrids with enhanced electrocatalytic performances. Electrochem Commun 9:1629–1634
24. Li CM, Zang JF, Zhan DP, Chen W, Sun CQ, Teo AL, Chua YT, Lee VS, Moochhala SM (2006) Electrochemical detection of nitric oxide on a SWCNT/RTIL composite gel microelectrode. Electroanalysis 18:713–718
25. He Q, Zheng DY, Hu SS (2009) Development and application of a nano-alumina based nitric oxide sensor. Microchim Acta 164:459–464
26. Milsom EV, Novak J, Oyama M, Marken F (2007) Electrocatalytic oxidation of nitric oxide at TiO_2-Au nanocomposite film electrodes. Electrochem Commun 9:436–442
27. Guo L, Huang QJ, Li XY, Yang SH (2006) PVP-coated iron nanocrystals: anhydrous synthesis, characterization, and electrocatalysis for two species. Langmuir 22:7867–7872
28. Wang HY, Huang YG, Tan Z, Hu XY (2004) Fabrication and characterization of copper nanoparticle thin-films and the electrocatalytic behavior. Anal Chim Acta 526:13–17
29. Lei CH, Wollenberger U, Bistolas N, Guiseppi-Elie A, Scheller FW (2002) Electron transfer of hemoglobin at electrodes modified with colloidal clay nanoparticles. Anal Bioanal Chem 372:235–239
30. Xu JH, Hu CG, Ji YP, Hu SS (2009) Ultrathin gold film deposited on human hair: derivation from nanoparticles and applications as microsensors. Electrochem Commun 11:764–767
31. Thangavel S, Ramaraj R (2008) Polymer membrane stabilized gold nanostructures modified electrode and its application in nitric oxide detection. J Phys Chem C 112:19825–19830
32. Li YJ, Liu C, Yang MH, He Y, Yeung ES (2008) Large-scale self-assembly of hydrophilic gold nanoparticles at oil/water interface and their electro-oxidation for nitric oxide in solution. J Electroanal Chem 622:103–108
33. Zhang JD, Oyama M (2005) Gold nanoparticle arrays directly grown on nanostructured indium tin oxide electrodes: characterization and electroanalytical application. Anal Chim Acta 540:299–306
34. Gu HY, Lu SY, Jiang QY, Yu CM, Li GX, Chen HY (2006) A novel nitric oxide cellular biosensor based on red blood cells immobilized on gold nanoparticles. Anal Lett 39:2849–2859
35. Daniel MC, Astruc D (2004) Gold nanoparticles: assembly, supramolecular chemistry, quantum-size-related properties, and applications toward biology, catalysis, and nanotechnology. Chem Rev 104:293–346
36. Brown KR, Fox AP, Natan MJ (1996) Morphology-dependent electrochemistry of cytochrome *c* at Au colloid-modified SnO_2 electrodes. J Am Chem Soc 118:1154–1157
37. Grabar KC, Freeman RG, Hommer MB, Natan MJ (1995) Preparation and characterization of Au colloid monolayers. Anal Chem 67:735–743
38. Luo XL, Xu JJ, Zhang Q, Yang GJ, Chen HY (2005) Electrochemically deposited chitosan hydrogel for horseradish peroxidase immobilization through gold nanoparticles self-assembly. Biosens Bioelectron 21:190–196
39. Yang YH, Yang HF, Yang MH, Liu YL, Shen GL, Yu RQ (2004) Amperometric glucose biosensor based on a surface treated nanoporous ZrO_2/chitosan composite film as immobilization matrix. Anal Chim Acta 525:213–220

40. Fahnestock KJ, Manesse M, McIlwee HA, Schauer CL, Boukherroub R, Szunerits S (2009) Selective detection of hexachromium ions by localized surface plasmon resonance measurements using gold nanoparticles/chitosan composite interfaces. Analyst 5:881–886
41. McIlwee HA, Schauer CL, Praig VG, Boukherroub R, Szunerits S (2008) Thin chitosan films as a platform for SPR sensing of ferric ions. Analyst 5:673–677
42. Guo SJ, Wang EK (2007) Synthesis and electrochemical applications of gold nanoparticles. Anal Chim Acta 598:181–192
43. Butler AR, Williams DLH (1993) The physiological role of nitric oxide. Chem Soc Rev 22:233–241
44. Lee Y, Kim J (2007) Simultaneous electrochemical detection of nitric oxide and carbon monoxide generated from mouse kidney organ tissues. Anal Chem 79:7669–7675
45. Luo XL, Xu JJ, Du Y, Chen HY (2004) A glucose biosensor based on chitosan–glucose oxidase–gold nanoparticles biocomposite formed by onestep electrodeposition. Anal Biochem 334:284–289
46. Xue MH, Xu Q, Zhou M, Zhu JJ (2006) In situ immobilization of glucose oxidase in chitosan–nanoparticle hybrid film on Prussian Blue modified for high-sensitivity glucose detection. Electrochem Commun 8:1468–1474
47. Feng D, Wang F, Chen ZL (2009) Electrochemical glucose sensor based on one-step construction of gold nanoparticle-chitosan composite film. Sens Actuators B-Chem 138:539–544
48. Katz E, Willner I, Wang J (2004) Electroanalytical and bioelectroanalytical systems based on metal and semiconductor nanoparticles. Electroanalysis 16:19–44
49. Bachmann S, Mundel P (1994) Nitric oxide in the kidney: synthesis, localization, and function. Am J Kidney Dis 24:112–129
50. Lahera V, Navarro CJ, Cachofeiro V, García-Estañ J, Ruilope LM (1997) Nitric oxide, the kidney, and hypertension. Am J Hypertens 10:129–140
51. Peng YF, Hu CG, Zheng DY, Hu SS (2008) A sensitive nitric oxide microsensor based on PBPB composite film-modified carbon fiber microelectrode. Sens Actuators B-Chem 133:571–576
52. Peng YF, Ji YP, Zheng DY, Hu SS (2009) In situ monitoring of nitric oxide release from rat kidney at poly(eosin b)-ionic liquid composite-based electrochemical sensors. Sens Actuators B-Chem 137:656–661
53. Lee Y, Yang J, Rudich SM, Schreiner RJ, Meyerhoff ME (2004) Improved planar amperometric nitric oxide sensor based on platinized platinum anode. 2. direct real-time measurement of NO generated from porcine kidney slices in the presence of l-arginine, l-arginine polymers, and protamine. Anal Chem 76:545–551
54. Yu A, Liang Z, Cho J, Caruso F (2003) Nanostructured electrochemical sensor based on dense gold nanoparticle films. Nano Lett 3:1203–1207